# Supplementary Information

# Enhancing Surface Activity and Durability in Triple Conducting Electrode for Protonic Ceramic Electrochemical Cells

Shuanglin Zheng[1], Wei Wu[2], Yuchen Zhang[2], Zeyu Zhao[2], Chuancheng Duan[3], Saroj Karki[1], Hanping Ding[1,*]

[1] School of Aerospace and Mechanical Engineering, University of Oklahoma, Norman, OK 73019 USA.

[2] Energy and Environment Science & Technology, Idaho National Laboratory, Idaho Falls, ID 83415 USA.

[3] Department of Chemical Engineering, University of Utah, Salt Lake City, UT 84112 USA

Correspondence authors' email: hding@ou.edu

**This PDF file includes:**

**Equation. S1.**

Equation. S1**.** The relationship between the rate of a chemical reaction and the activation energy is described by the Arrhenius equation:

$$R_O = A_O \exp(-\frac{E_{a,o}}{\kappa_B T}) \quad (1)$$

$$R_p = A_p \exp(-\frac{E_{a,p}}{\kappa_B T}) \quad (2)$$

where $A$ is the pre-exponent factor; $E_a$ is the activation energy; the subscripts *o* and *p* denote the ohmic and polarization resistance, respectively; $\kappa_B$ is the Boltzmann constant and $T$ is the absolute temperature in Kelvin.

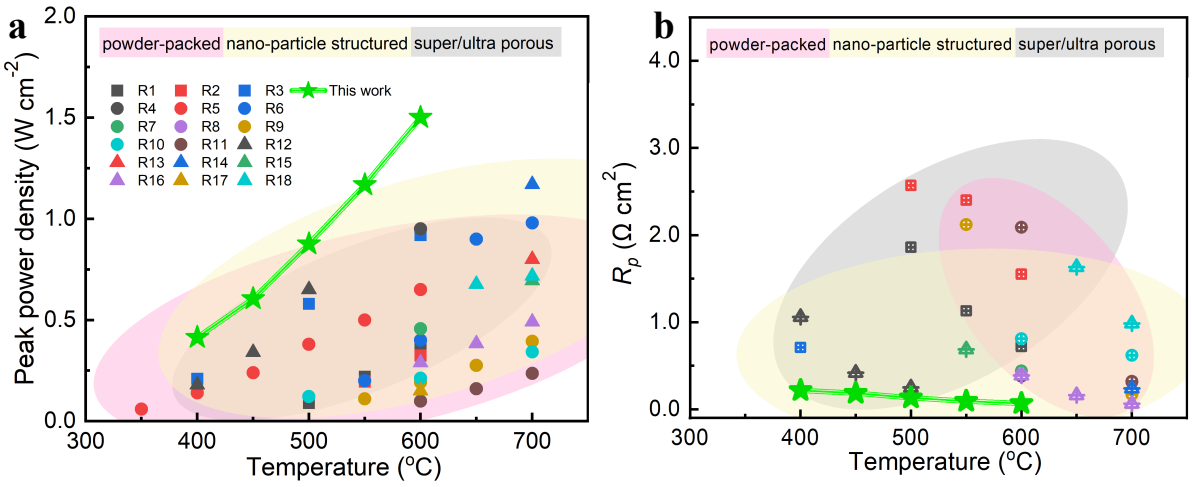


**Fig. S1. Highly enhanced electrochemical performance of PCEC with nano-architecture ultra-porous (NAUP) PNC73 electrode. a** Comparison on peak power density of NAUP-PNC73 (this work) in fuel cell mode with the literature results. The NAUP-PNC73 full cells are readily fabricated in this work using self-structured mesh to achieve ultra-porous configuration. Thus, another similar fabrication methods: powder-packed electrode; nano-particle electrode and super/ultra porous electrode, are used to provide a more distinct contrast. The temperature range of all conducted tests was 350-700 °C[1–18]. **b** Polarization resistance ($R_p$) of NAUP-PNC73 under OCV conditions in comparison with the representative results.

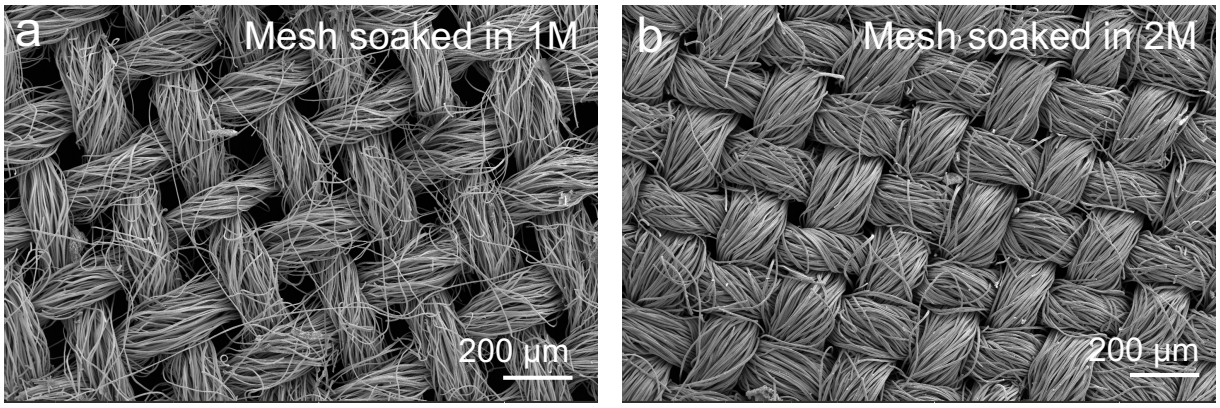


**Fig. S2. SEM images of NAUP-PNC mesh-structured electrode. a** Mesh soaked in 1M PNC73 solution. **b** Mesh soaked in 2M PNC73 solution.

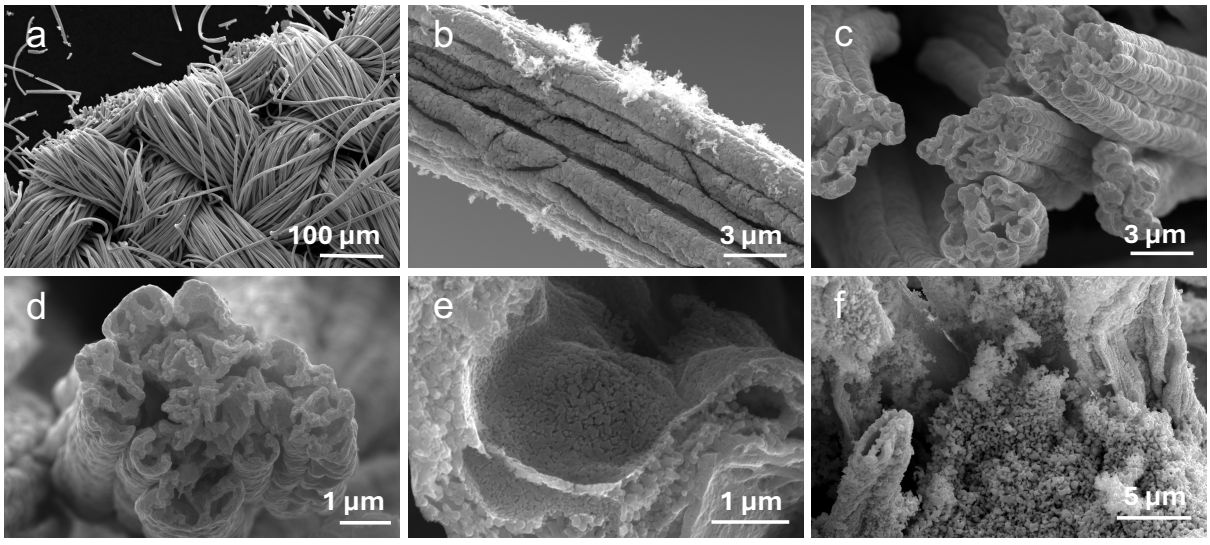


**Fig. S3. SEM images** of **a** NAUP-PNC mesh-structured electrode edges. **b** one NAUP-PNC mesh-structured electrode fiber. **c** cross sections of several NAUP-PNC mesh-structured electrode fibers. **d** the cross section of one NAUP-PNC mesh-structured electrode fiber. **e** the inner wall of one NAUP-PNC mesh-structured electrode fiber. **f** bonding relationship between NAUP-PNC mesh-structured electrode fibers and PNC73 ink.

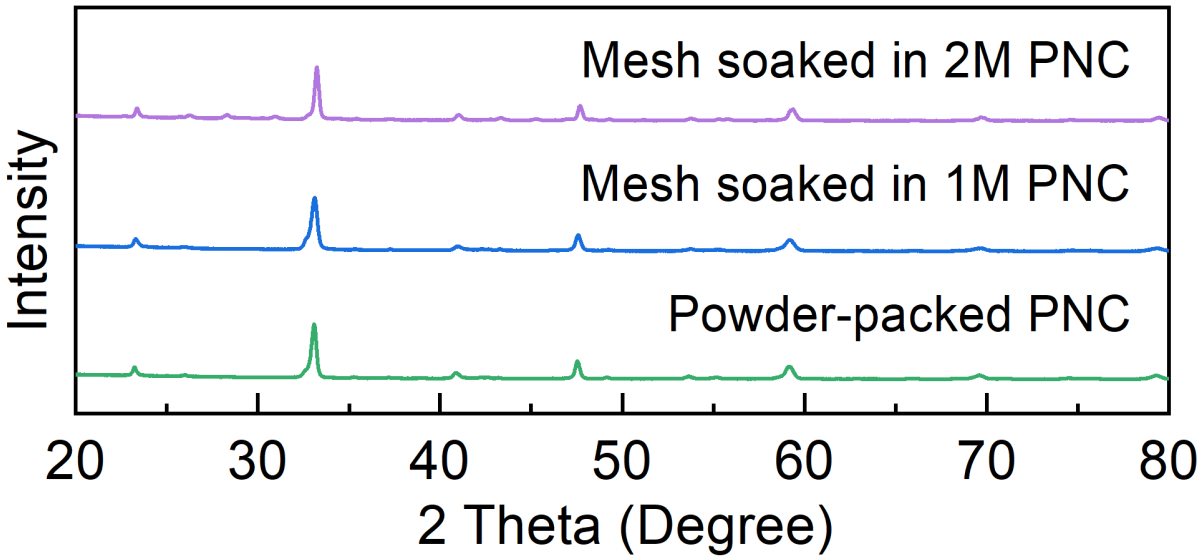


**Fig. S4. XRD results of powder-packed PNC electrode.** NAUP-PNC mesh-structured electrode soaked in 1M PNC73 solution and soaked in 2M PNC73 solution, respectively. All showed the pure phase.

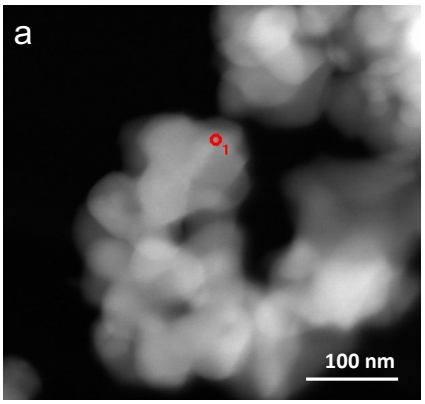


b

| Element | Weight % | Atomic % | Uncert. % | Correction | k-Factor |
|---|---|---|---|---|---|
| O(K) | 4.72 | 23.65 | 0.26 | 0.51 | 1.921 |
| Co(K) | 16.55 | 22.48 | 0.39 | 0.99 | 1.441 |
| Ni(K) | 11.50 | 15.68 | 0.33 | 0.99 | 1.453 |
| Pr(L) | 67.20 | 38.17 | 0.88 | 0.99 | 3.113 |

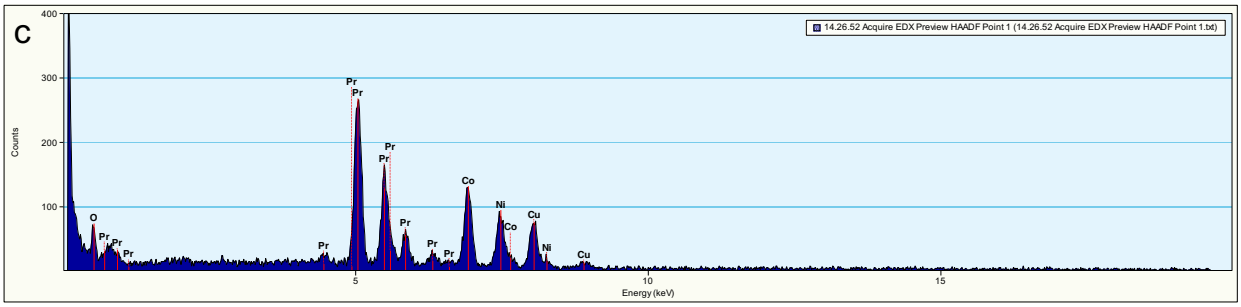


**Fig. S5: TEM characterization of NAUP-PNC oxygen electrode. a** HAADF image of NAUP-PNC nanoparticles. **b** Table of elemental amounts in percentages on site 1. **c** EDS spectra of HAADF site 1.

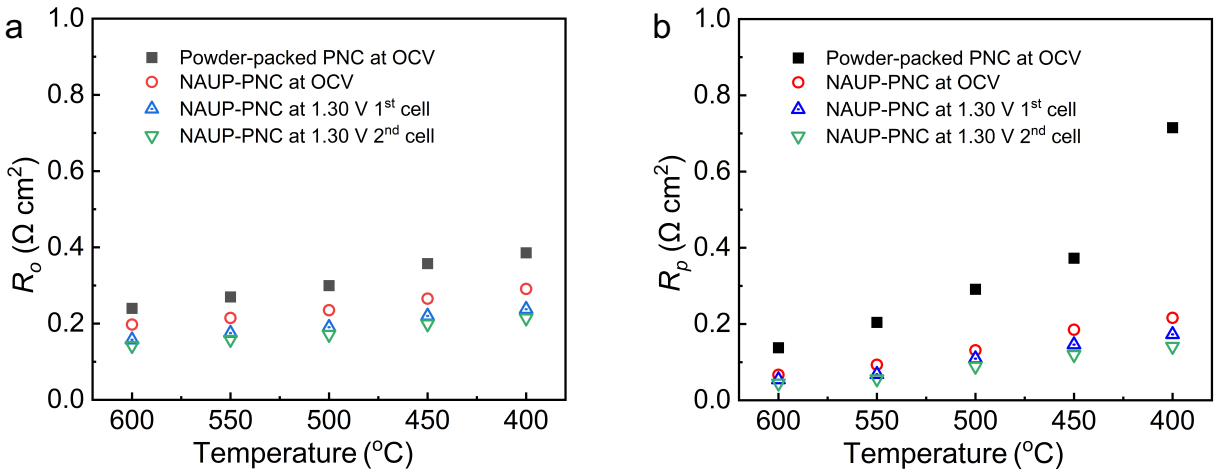


c

| Powder-packed PNC at OCV | $R_o$ (Ω cm$^2$) | $R_p$ (Ω cm$^2$) | Standard deviation for $R_p$ | NAUP-PNC at OCV | $R_o$ (Ω cm$^2$) | $R_p$ (Ω cm$^2$) | Standard deviation for $R_p$ | NAUP-PNC at 1.30 V | $R_o$ (Ω cm$^2$) | $R_p$ (Ω cm$^2$) | Standard deviation for $R_p$ |
|---|---|---|---|---|---|---|---|---|---|---|---|
| 600 °C | 0.2012 | 0.1767 | 0.00174 | 600 °C | 0.1976 | 0.0668 | 0.00155 | 600 °C | 0.1577 | 0.0530 | 0.00157 |
| 550 °C | 0.2641 | 0.3277 | 0.00146 | 550 °C | 0.2241 | 0.0840 | 0.00143 | 550 °C | 0.1752 | 0.0682 | 0.00134 |
| 500 °C | 0.3515 | 0.7146 | 0.00132 | 500 °C | 0.2373 | 0.1278 | 0.00162 | 500 °C | 0.1904 | 0.1091 | 0.00144 |
| 450 °C | 0.4713 | 1.6939 | 0.00142 | 450 °C | 0.2508 | 0.1997 | 0.00147 | 450 °C | 0.2202 | 0.1460 | 0.00124 |
| 400 °C | 0.4952 | 1.9105 | 0.00159 | 400 °C | 0.2682 | 0.2387 | 0.00167 | 400 °C | 0.2376 | 0.1729 | 0.00133 |

**Fig. S6. Comparison of $R_o$ (a) and $R_p$ (b)** between NAUP-PNC cells and powder-packed PNC cells under both SOFC and SOEC modes at 400-600 °C. **c** Resistance value with corresponding standard deviations.

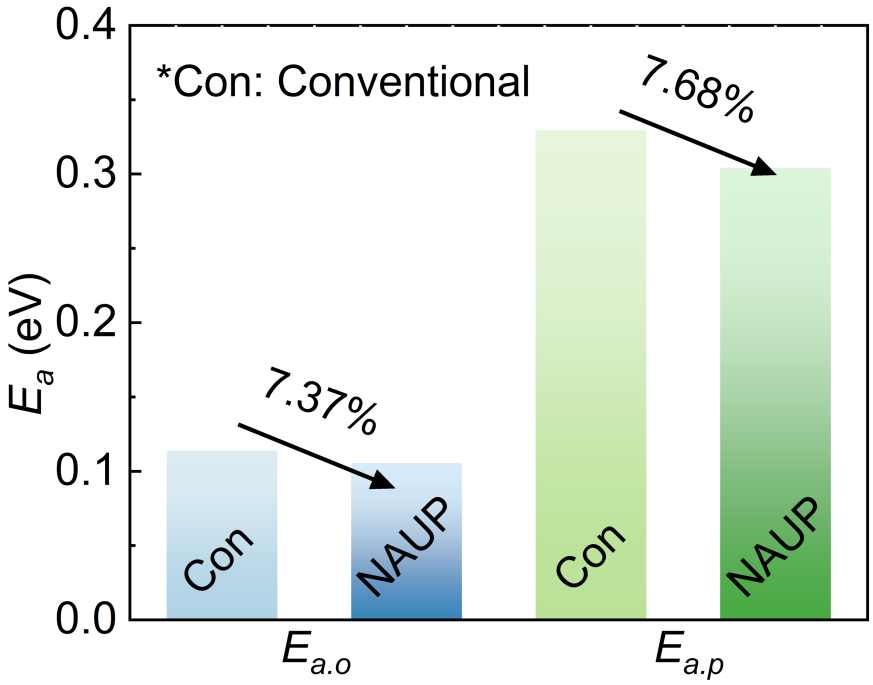


**Fig. S7:** Comparison between $E_a$ from ohmic resistance and $E_a$ from polarization resistance.

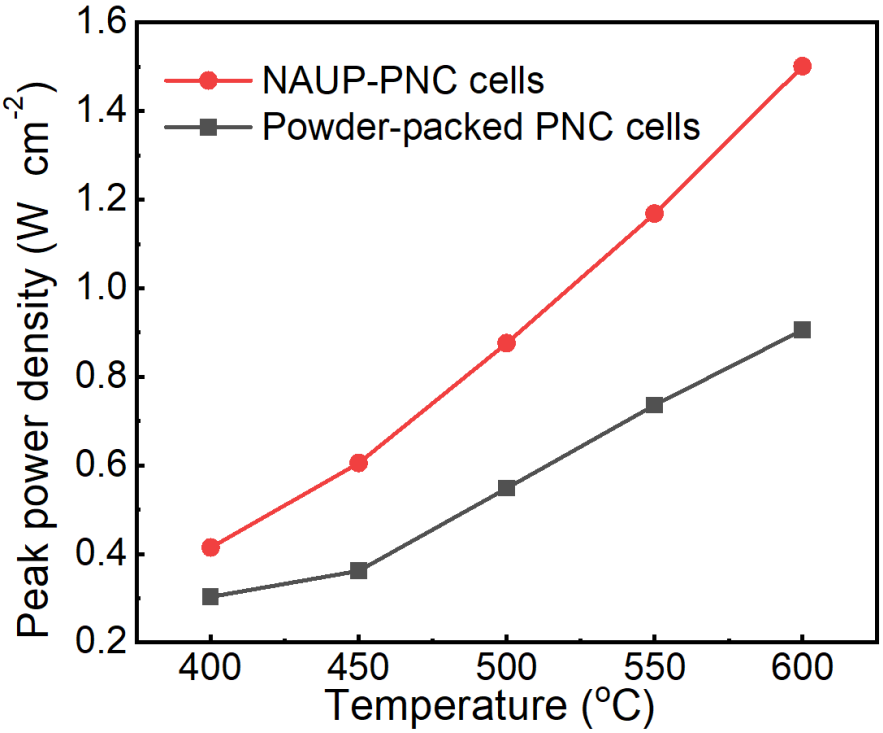


**Fig. S8. Comparison of peak power density** between NAUP-PNC cells and powder-packed PNC cells under SOFC mode at 400-600 ºC.

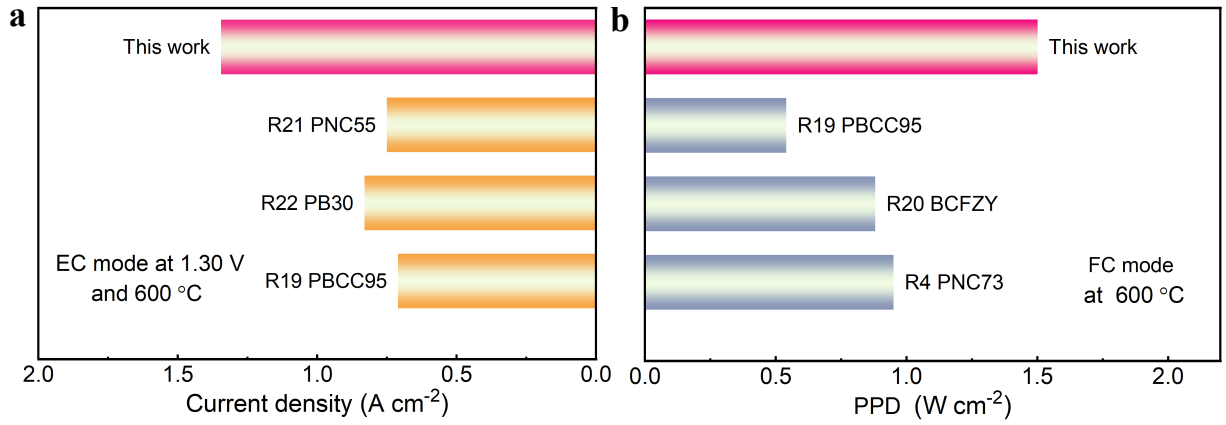


**Fig. S9. Comparison of NAUP-PNC73 full cell performances in both FC and EC modes with some recent literatures**[4,19–22]**.** BCFZY, $BaCo_{0.4}Fe_{0.4}Zr_{0.1}Y_{0.1}O_{3-\delta}$; PNC73, $PrNi_{0.7}Co_{0.3}O_{3-\delta}$; PNC55, $PrNi_{0.5}Co_{0.5}O_{3-\delta}$; PB30, $Pr_{1.7}Ba_{0.3}NiO_{4+\delta}$; PBCC95, $(PrBa_{0.8}Ca_{0.2})_{0.95}Co_2O_{6-\delta}$.

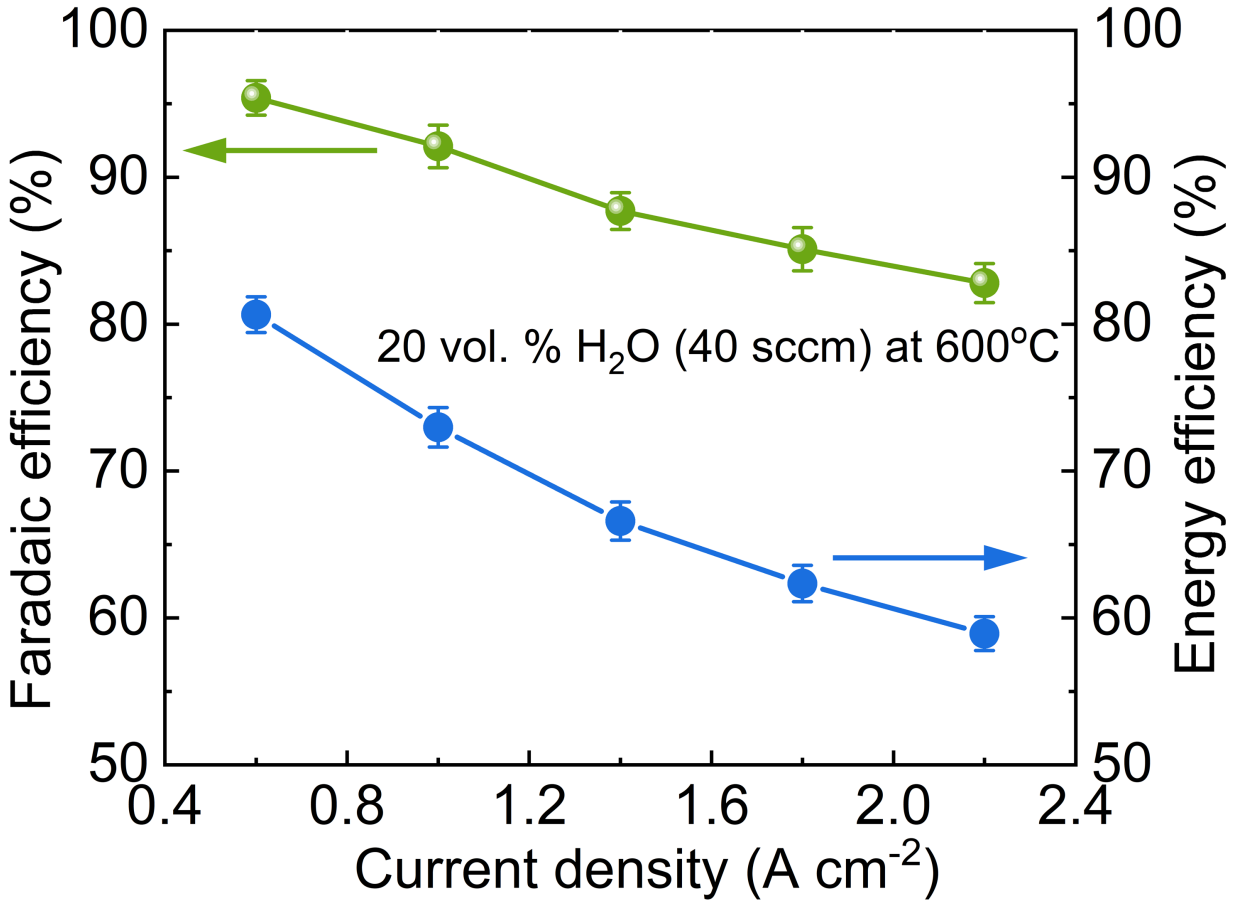


| Current density (A $cm^{-2}$) | FE (%) | Standard deviation of FE | EE (%) | Standard deviation of EE |
|---|---|---|---|---|
| 0.60 | 95.4 | ±1.17 | 80.6 | ±1.22 |
| 1.00 | 92.1 | ±1.45 | 72.9 | ±1.34 |
| 1.40 | 87.7 | ±1.25 | 66.6 | ±1.30 |
| 1.80 | 85.1 | ±1.47 | 62.3 | ±1.24 |
| 2.20 | 82.8 | ±1.33 | 58.9 | ±1.15 |

**Fig. S10.** Faradic efficiency (FE, %) and Energy efficiency (EE, %) of NAUP-PNC full cells in electrolysis mode at 600°C (top). Table of statistical standard deviations for FE and EE (bottom). Each test was conducted for six times to get the statistical standard deviations, presented as error bars.

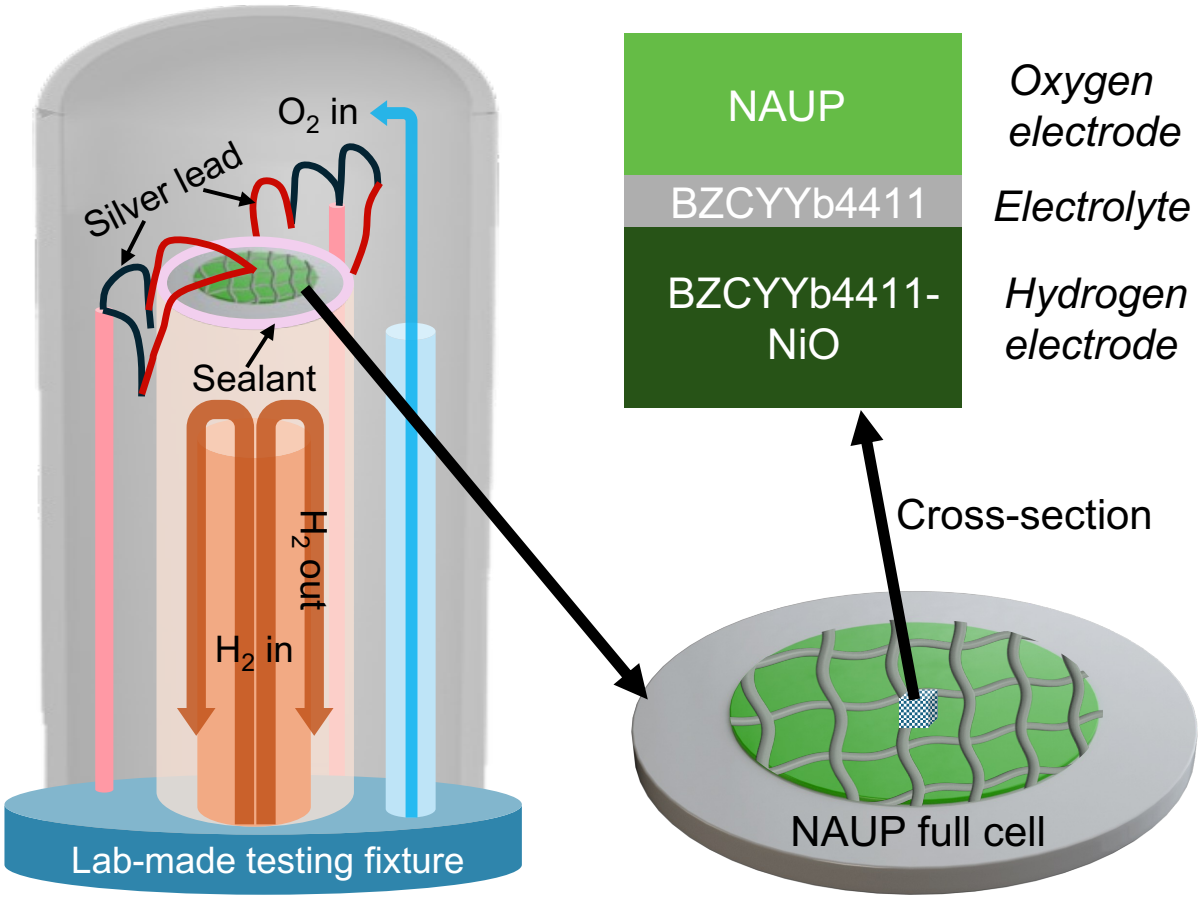


**Fig. S11.** Lab-made testing fixture used in this work.

| PPD (W $cm^{-2}$) | Temperature (°C) | | | | | | | | ***Experimental condition*** | Fabrication |
|---|---|---|---|---|---|---|---|---|---|---|
| | 700 | 650 | 600 | 550 | 500 | 450 | 400 | 350 | | |
| This work | - | - | 1.50 | 1.17 | 0.88 | 0.61 | 0.41 | - | *Under $H_2/O_2$* | NAUP |
| Ref. 1 | - | - | 0.36 | 0.22 | 0.09 | - | - | - | *A steam partial pressure of 12%/Pure $H_2$/FC at 0.7 V* | 3D self-architectured steam electrode |
| Ref. 2 | - | - | 0.33 | 0.20 | - | - | - | - | *Cathode: 75% $CO_2$+25%$O_2$/Anode : Ar* | 3D architectured electrode |
| Ref. 3 | - | - | 0.92 | - | 0.58 | - | 0.21 | - | *Cathode: pure $O_2$/Anode: pure $H_2$* | 3D engineering electrode |
| Ref. 4 | - | - | 0.95 | - | - | - | - | - | *Wet $H_2$ (3% steam) on the fuel side and pure oxygen on the oxygen side* | Powder-packed electrode |
| Ref. 5 | - | - | 0.65 | 0.50 | 0.38 | 0.24 | 0.14 | 0.06 | *Under $H_2$/air* | Powder-packed electrode |
| Ref. 6 | 1.30 | 0.90 | 0.40 | 0.20 | - | - | - | - | *Under $H_2/O_2$* | Powder-packed electrode |
| Ref. 7 | - | - | 0.46 | - | - | - | - | - | *Under $H_2/O_2$* | Powder-packed electrode |
| Ref. 8 | - | - | - | - | - | - | - | - | - | Powder-packed electrode |
| Ref. 9 | 0.40 | 0.28 | 0.19 | 0.11 | - | - | - | - | *Under $H_2$/air* | Powder-packed electrode |
| Ref. 10 | 0.34 | - | 0.21 | - | 0.12 | - | - | - | *Humidified $H_2/O_2$* | Powder-packed electrode |
| Ref. 11 | 0.24 | 0.16 | 0.10 | - | - | - | - | - | *Humidified hydrogen (~3% $H_2O$) /$O_2$* | Powder-packed electrode |
| Ref. 12 | - | - | - | - | 0.65 | 0.34 | 0.18 | - | *Humidified hydrogen (~3% $H_2O$) /air* | Nano-network electrode |
| Ref. 13 | 0.80 | - | - | - | - | - | - | - | *Under $H_2/O_2$* | Nano-tailoring electrode |
| Ref. 14 | 1.37 | - | - | - | - | - | - | - | *Humidified hydrogen (~6% $H_2O$) /air* | Nanocatalyst electrode |
| Ref. 15 | 0.70 | - | - | - | - | - | - | - | *Humidified hydrogen (~3% $H_2O$) /air* | Infiltrated nano-electrode |
| Ref. 16 | 0.49 | 0.38 | 0.29 | - | - | - | - | - | *Humidified hydrogen (~3% $H_2O$) /air* | Infiltrated multiscale electrode |
| Ref. 17 | - | - | 0.15 | - | - | - | - | - | *Humidified hydrogen (~3% $H_2O$) /air* | Nanostructured electrode |
| Ref. 18 | 0.72 | 0.68 | - | - | - | - | - | - | *Humidified hydrogen (~3% $H_2O$) /air* | Nanostructured electrode |

**Table. S1.** Comparison of peak power density between this work and other literature results.

| $R_p$ ($\Omega$ cm$^2$) | Temperature (°C) | | | | | | | | ***Experimental condition*** | Fabrication |
|---|---|---|---|---|---|---|---|---|---|---|
| | 700 | 650 | 600 | 550 | 500 | 450 | 400 | 350 | | |
| This work | - | - | 0.07 | 0.09 | 0.13 | 0.19 | 0.22 | - | *Under $H_2/O_2$ /at OCV* | NAUP |
| Ref. 1 | - | - | 0.72 | 1.13 | 1.86 | - | - | - | *A steam partial pressure of 12%/Pure $H_2$/FC at OCV* | 3D self-architectured steam electrode |
| Ref. 2 | - | - | 1.55 | 2.10 | 2.57 | - | - | - | *Cathode: 75% $CO_2$+25%$O_2$/Anode : Ar/at OCV* | 3D architectured electrode |
| Ref. 3 | - | - | - | - | - | - | 0.71 | - | *Cathode: pure $O_2$/Anode: pure $H_2$ /at OCV* | 3D engineering electrode |
| Ref. 4 | - | - | 0.38 | - | - | - | - | - | *Wet $O_2$ (3% steam) at OCV* | Powder-packed electrode |
| Ref. 5 | - | - | - | - | - | - | - | - | - | Powder-packed electrode |
| Ref. 6 | - | - | - | - | - | - | - | - | - | Powder-packed electrode |
| Ref. 7 | - | - | 0.44 | - | - | - | - | - | *Under $H_2/O_2$ /at OCV* | Powder-packed electrode |
| Ref. 8 | 0.31 | - | 0.40 | - | - | - | - | - | *Steam in anode: 0.4 atm* | Powder-packed electrode |
| Ref. 9 | 0.17 | - | - | 2.12 | - | - | - | - | *Under $H_2$/air /at OCV* | Powder-packed electrode |
| Ref. 10 | 0.62 | - | 0.81 | - | - | - | - | - | *Humidified $H_2/O_2$ /at OCV* | Powder-packed electrode |
| Ref. 11 | 0.32 | - | 2.09 | - | - | - | - | - | *Humidified hydrogen (~3% $H_2O$) /$O_2$/at OCV* | Powder-packed electrode |
| Ref. 12 | - | - | - | - | 0.25 | 0.42 | 1.06 | - | *Humidified hydrogen (~3% $H_2O$) /air /at OCV* | Nano-network electrode |
| Ref. 13 | - | - | - | - | - | - | - | - | - | Nano-tailoring electrode |
| Ref. 14 | 0.24 | - | - | - | - | - | - | - | *Humidified hydrogen (~6% $H_2O$) /air /at OCV* | Nanocatalyst electrode |
| Ref. 15 | - | - | - | 0.67 | - | - | - | - | *Humidified hydrogen (~3% $H_2O$) /air /at OCV* | Infiltrated nano-electrode |
| Ref. 16 | 0.06 | 0.16 | 0.39 | - | - | - | - | - | *Humidified hydrogen (~3% $H_2O$) /air /at OCV* | Infiltrated multiscale electrode |
| Ref. 17 | - | - | - | - | - | - | - | - | - | Nanostructured electrode |
| Ref. 18 | 0.99 | 1.63 | - | - | - | - | - | - | *Humidified hydrogen (~3% $H_2O$) /air /at OCV* | Nanostructured electrode |

**Table. S2.** Comparison of $R_p$ between this work and other literature results.

| $R_o$ | $E_a$ (eV) | Standard deviation |
|---|---|---|
| Powder-packed PNC at OCV | 0.1139 | ±0.01399 |
| NAUP-PNC at OCV | 0.1055 | ±0.01197 |
| NAUP-PNC at 1.30 V 1st cell | 0.1059 | ±0.01323 |
| NAUP-PNC at 1.30 V 2nd cell | 0.1064 | ±0.01378 |

**Table. S3.** Calculated $E_{a,o}$ with standard errors of NAUP-PNC cells and powder-packed PNC cells under both SOFC and SOEC modes.

| $R_p$ | $E_a$ (eV) | Standard deviation |
|---|---|---|
| Powder-packed PNC at OCV | 0.32935 | ±0.01807 |
| NAUP-PNC at OCV | 0.30406 | ±0.01371 |
| NAUP-PNC at 1.30 V 1st cell | 0.30768 | ±0.01742 |
| NAUP-PNC at 1.30 V 2nd cell | 0.30817 | ±0.01728 |

**Table. S4.** Calculated $E_{a,p}$ with standard errors of NAUP-PNC cells and powder-packed PNC cells under both SOFC and SOEC modes.

| NAUP-PNC cells | | | | | |
|---|---|---|---|---|---|
| Temperature (°C) | 400 | 450 | 500 | 550 | 600 |
| Peak power density (W $cm^{-2}$) | 0.4140 | 0.6055 | 0.8762 | 1.1684 | 1.5012 |

| Powder-packed PNC cells | | | | | |
|---|---|---|---|---|---|
| Temperature (°C) | 400 | 450 | 500 | 550 | 600 |
| Peak power density (W $cm^{-2}$) | 0.3031 | 0.3619 | 0.5481 | 0.7364 | 0.9056 |

**Table. S5.** Comparison of peak power density between NAUP-PNC cells (top) and powder-packed PNC cells (bottom) under SOFC mode at 400-600 °C.

| NAUP-PNC ells | | | | | |
|---|---|---|---|---|---|
| Temperature (°C) | 400 | 450 | 500 | 550 | 600 |
| Current density (A $cm^{-2}$) | -0.6512 | -1.5245 | -2.4985 | -3.8627 | -5.0423 |

| Powder-packed PNC cells | | | | | |
|---|---|---|---|---|---|
| Temperature (°C) | 400 | 450 | 500 | 550 | 600 |
| Current density (A $cm^{-2}$) | -0.4932 | -1.1012 | -1.5321 | -2.6021 | -3.3605 |

**Table. S6.** Comparison of current density of NAUP-PNC cells (top) and powder-packed PNC cells (bottom) under SOEC mode at 400-600 °C.

| Relative humidity (vol.% $H_2O$) | 3 | 10 | 20 | 30 |
|---|---|---|---|---|
| Current density (A $cm^{-2}$) | -4.0265 | -4.5124 | -5.0397 | -4.7397 |

| Gas flow rate (sccm) | 10 | 20 | 40 | 60 |
|---|---|---|---|---|
| Current density (A $cm^{-2}$) | -4.2151 | -4.6001 | -5.0258 | -4.8225 |

**Table. S7.** Comparison of current density of NAUP-PNC cells in terms of relative humidity (top) and gas flow rate (bottom) under SOEC mode at 600 ºC.

| PPD (W $cm^{-2}$) | | | | |
|---|---|---|---|---|
| Ref. | R4<br>PNC73 | R20<br>BCFZY | R19<br>PBCC95 | This work |
| Conditions | $H_2$-Humidified $O_2$ (50% $H_2O$) | Humidified $H_2$ (3% $H_2O$) -Humidified $O_2$ (3% $H_2O$) | Humidified $H_2$ (3% $H_2O$) -$O_2$ | $H_2$-Humidified $O_2$ (3% $H_2O$) |
| PPD (W $cm^{-2}$) | 0.95 | 0.88 | 0.54 | 1.50 |

| CD at 1.30V (A $cm^{-2}$) | | | | |
|---|---|---|---|---|
| Ref. | R22<br>PB30 | R19<br>PBCC95 | R21<br>PNC55 | This work |
| Conditions | $H_2$-Humidified $O_2$ (60% $H_2O$) | Humidified $H_2$ (3% $H_2O$) -Humidified $O_2$ (20% $H_2O$) | Humidified $H_2$ (3% $H_2O$) -Humidified $O_2$ (50% $H_2O$) | $H_2$-Humidified $O_2$ (20% $H_2O$) |
| CD at 1.30V (A $cm^{-2}$) | 0.83 | 0.71 | 0.75 | 1.35 |

**Table. S8.** Comparison of peak power density and current density for the reference data in Fig. S9.

| *X*th | $R_o$ (Ω cm$^2$) | $R_t$ (Ω cm$^2$) | $R_p$ (Ω cm$^2$) |
|---|---|---|---|
| 1st | 0.1577 | 0.2099 | 0.05220 |
| 2nd | 0.1579 | 0.2084 | 0.05055 |
| 3rd | 0.1582 | 0.2098 | 0.05158 |
| 4th | 0.1586 | 0.2116 | 0.05304 |
| 5th | 0.1592 | 0.2095 | 0.05029 |
| 6th | 0.1583 | 0.2085 | 0.05026 |
| 7th | 0.1572 | 0.2093 | 0.05214 |
| 8th | 0.1576 | 0.2084 | 0.05083 |
| 9th | 0.1574 | 0.2081 | 0.05061 |
| 10th | 0.1558 | 0.2091 | 0.05330 |
| 11th | 0.1554 | 0.2099 | 0.05450 |
| 12th | 0.1571 | 0.2095 | 0.05235 |
| 13th | 0.1563 | 0.2100 | 0.05368 |
| 14th | 0.1535 | 0.2095 | 0.05599 |
| 15th | 0.1535 | 0.2095 | 0.05596 |
| 16th | 0.1548 | 0.2095 | 0.05465 |
| 17th | 0.1524 | 0.2109 | 0.05851 |
| 18th | 0.1547 | 0.2079 | 0.05313 |
| 19th | 0.1586 | 0.2116 | 0.05304 |
| 20th | 0.1554 | 0.2087 | 0.05336 |

**Table. S9.** Results of $R_o$, $R_t$ and $R_p$ of NAUP-PNC cells at 1.30 V and 600 ºC for 20 cycles.

| Time (h) | Current density (A $cm^{-2}$) | | | Mean % |
|---|---|---|---|---|
| | -Value | Difference | % of degradation | |
| 0 | 1.2889 | | | |
| 10 | 1.2763 | 0.0126 | 0.98 | |
| 20 | 1.2632 | 0.0131 | 1.03 | 1.03 |
| 30 | 1.2499 | 0.0133 | 1.05 | |
| 40 | 1.2369 | 0.0130 | 1.04 | |
| 50 | 1.2239 | 0.0130 | 1.05 | |
| Altering applied voltage from 1.30 V to 1.40 V | | | | |
| 50 | 1.9958 | | | |
| 60 | 1.9729 | 0.0230 | 1.15 | |
| 70 | 1.9482 | 0.0247 | 1.25 | 1.24 |
| 80 | 1.9242 | 0.0240 | 1.23 | |
| 90 | 1.9002 | 0.0241 | 1.25 | |
| 100 | 1.8753 | 0.0249 | 1.31 | |

**Table. S10.** % of degradation calculation on current density of NAUP-PNC cells at 1.30 V/1.40 V and 600 ºC for 100 hours.

| Time (h) | Current density (A $cm^{-2}$) | | | Mean % |
|---|---|---|---|---|
| | Mode | Standard deviation | % of degradation | |
| 0-10 | | 0.02036 | 1.69 | |
| 20-30 | | 0.02168 | 1.83 | |
| 40-50 | SOEC | 0.02244 | 1.93 | 1.87 |
| 60-70 | | 0.02144 | 1.88 | |
| 80-90 | | 0.02204 | 1.97 | |
| 10-20 | | 0.02823 | 1.48 | |
| 30-40 | | 0.02969 | 1.58 | |
| 50-60 | SOFC | 0.02977 | 1.61 | 1.55 |
| 70-80 | | 0.02893 | 1.59 | |
| 90-100 | | 0.02668 | 1.49 | |

**Table. S11.** % of degradation calculation on current density of NAUP-PNC cells for reversible tests at 600 ºC for 100 hours.

| *X*th | Current density (A $cm^{-2}$) | | | Mean % |
|---|---|---|---|---|
| | Voltage (V) | Standard deviation | % of degradation | |
| 1 | | 0.05634 | 1.85 | |
| 2 | | 0.05410 | 1.81 | |
| 3 | | 0.05605 | 1.91 | |
| 4 | | 0.05239 | 1.82 | |
| 5 | | 0.05257 | 1.86 | |
| 6 | | 0.05104 | 1.84 | |
| 7 | 1.50 | 0.05935 | 2.18 | 1.94 |
| 8 | | 0.05620 | 2.11 | |
| 9 | | 0.05423 | 2.08 | |
| 10 | | 0.04902 | 1.92 | |
| 11 | | 0.04732 | 1.89 | |
| 12 | | 0.04889 | 1.99 | |
| 13 | | 0.04623 | 1.92 | |

**Table. S12.** % of degradation calculation on current density of NAUP-PNC cells for transient tests (step-voltage based) at 1.50 V and 600 ºC.

| *X*th | Current density (A $cm^{-2}$) | | | Mean % |
|---|---|---|---|---|
| | Voltage (V) | Standard deviation | % of degradation | |
| 1&2 | | 0.02270 | 1.35 | |
| 3&4 | | 0.02273 | 1.37 | |
| 5&6 | | 0.02176 | 1.33 | |
| 7&8 | | 0.02164 | 1.34 | |
| 9&10 | | 0.02023 | 1.27 | |
| 11&12 | | 0.01903 | 1.21 | |
| | 1.35 | | | 1.28 |
| 13&14 | | 0.01989 | 1.28 | |
| 15&16 | | 0.01856 | 1.21 | |
| 17&19 | | 0.01955 | 1.29 | |
| 19&20 | | 0.01959 | 1.31 | |
| 21&22 | | 0.01757 | 1.19 | |
| 23&24 | | 0.01823 | 1.25 | |

**Table. S13.** % of degradation calculation on current density of NAUP-PNC cells for transient tests (step-voltage based) at 1.35 V and 600 ºC.

| *X*th | Current density (A $cm^{-2}$) | | | Mean % |
|---|---|---|---|---|
| | Voltage (V) | Standard deviation | % of degradation | |
| 1 | | 0.00327 | 0.45 | |
| 2 | | 0.00304 | 0.42 | |
| 3 | | 0.00303 | 0.42 | |
| 4 | | 0.00352 | 0.49 | |
| 5 | | 0.00343 | 0.48 | |
| 6 | | 0.00313 | 0.44 | |
| | 1.20 | | | 0.45 |
| 7 | | 0.00318 | 0.45 | |
| 8 | | 0.00303 | 0.43 | |
| 9 | | 0.00358 | 0.51 | |
| 10 | | 0.00272 | 0.39 | |
| 11 | | 0.00306 | 0.44 | |
| 12 | | 0.00311 | 0.45 | |

**Table. S14.** % of degradation calculation on current density of NAUP-PNC cells for transient tests (step-voltage based) at 1.20 V and 600 ºC.

| *X*th | Current density (A $cm^{-2}$) | | | Mean % |
|---|---|---|---|---|
| | Voltage (V) | Standard deviation | % of degradation | |
| 1 | | 0.00722 | 0.24 | |
| 2 | | 0.04665 | 1.56 | |
| 3 | | 0.00393 | 0.13 | |
| 4 | | 0.03728 | 1.26 | |
| 5 | | 0.03791 | 1.30 | |
| 6 | | 0.01210 | 0.41 | |
| 7 | | 0.05000 | 1.69 | |
| 8 | 1.50 | 0.03888 | 1.33 | 1.07 |
| 9 | | 0.03888 | 1.32 | |
| 10 | | 0.07500 | 2.57 | |
| 11 | | 0.04155 | 1.39 | |
| 12 | | 0.03321 | 1.13 | |
| 13 | | 0.00118 | 0.04 | |
| 14 | | 0.01784 | 0.60 | |
| 15 | | 0.03333 | 1.12 | |

**Table. S15.** % of degradation calculation on current density of NAUP-PNC cells for transient tests (time-interval based) at 1.50 V and 600 ºC.

| *X*th | Current density (A $cm^{-2}$) | | | Mean % |
|---|---|---|---|---|
| | Voltage (V) | Standard deviation | % of degradation | |
| 1 | 1.20 | 0.00747 | 0.75 | 4.11 |
| 2 | | 0.00333 | 0.33 | |
| 3 | | 0.02334 | 2.34 | |
| 4 | | 0.00666 | 0.68 | |
| 5 | | 0.06167 | 6.38 | |
| 6 | | 0.08500 | 9.39 | |
| 7 | | 0.00500 | 0.51 | |
| 8 | | 0.06833 | 6.87 | |
| 9 | | 0.05000 | 5.40 | |
| 10 | | 0.01333 | 1.36 | |
| 11 | | 0.08500 | 8.59 | |
| 12 | | 0.05333 | 5.89 | |
| 13 | | 0.04000 | 4.17 | |
| 14 | | 0.08666 | 8.68 | |
| 15 | | 0.04000 | 4.39 | |
| 16 | | 0.02916 | 3.06 | |

**Table. S16.** % of degradation calculation on current density of NAUP-PNC cells for transient tests (time-interval based) at 1.20 V and 600 ºC.

| Voltage (V) | % of degradation | Mean % |
|---|---|---|
| 1.50 V | 1.07 | |
| | | 2.59 |
| 1.20 V | 4.11 | |

**Table. S17.** Mean % of degradation calculation on current density of NAUP-PNC cells for transient tests (time-interval based) at 600 ºC.

| *X*th | CD at SOFC (A $cm^2$) | CD at SOEC (A $cm^2$) | Temperature ($^oC$) |
|---|---|---|---|
| 1st | 4.68322 | -4.87872 | 600 |
| 2nd | 3.34564 | -2.94545 | 550 |
| 3rd | 3.09026 | -2.40625 | 500 |
| 4th | 3.28819 | -2.89412 | 550 |
| 5th | 4.58335 | -4.78633 | 600 |
| 6th | 3.21531 | -2.76239 | 550 |
| 7th | 2.92903 | -1.90668 | 500 |
| 8th | 2.95254 | -2.49223 | 550 |
| 9th | 4.4722 | -4.78633 | 600 |
| 10th | 2.78259 | -2.32329 | 550 |
| 11th | 2.76781 | -1.7373 | 500 |
| 12th | 2.66128 | -2.20302 | 550 |
| 13th | 4.47308 | -4.67502 | 600 |
| 14th | 2.52947 | -2.06924 | 550 |
| 15th | 2.40252 | -1.1122 | 500 |

**Table. S18.** Results of maximum current density of NAUP-PNC cells for thermal cycling tests.

| *X*th | $R_o$ (Ω cm$^2$) | $R_t$ (Ω cm$^2$) | $R_p$ (Ω cm$^2$) | Standard deviation for $R_p$ | Temperature ($^o$C) |
|---|---|---|---|---|---|
| 1st | 0.16555 | 0.22275 | 0.05720 | 0.00134 | 600 |
| 2nd | 0.18043 | 0.25075 | 0.07032 | 0.00115 | 550 |
| 3rd | 0.19417 | 0.30703 | 0.11286 | 0.00107 | 500 |
| 4th | 0.18049 | 0.25687 | 0.07638 | 0.00129 | 550 |
| 5th | 0.16531 | 0.22604 | 0.06073 | 0.00135 | 600 |
| 6th | 0.1806 | 0.2615 | 0.08090 | 0.00147 | 550 |
| 7th | 0.19399 | 0.31509 | 0.12110 | 0.00151 | 500 |
| 8th | 0.18176 | 0.26166 | 0.07990 | 0.00147 | 550 |
| 9th | 0.16625 | 0.22853 | 0.06228 | 0.00132 | 600 |
| 10th | 0.18162 | 0.2627 | 0.08108 | 0.00132 | 550 |
| 11th | 0.19703 | 0.32481 | 0.12778 | 0.00128 | 500 |
| 12th | 0.18127 | 0.26595 | 0.08468 | 0.00121 | 550 |
| 13th | 0.16689 | 0.23154 | 0.06465 | 0.00145 | 600 |
| 14th | 0.18162 | 0.26827 | 0.08665 | 0.00133 | 550 |
| 15th | 0.19725 | 0.33375 | 0.13650 | 0.00129 | 500 |

**Table. S19.** Results of $R_o$, $R_t$ and $R_p$ of NAUP-PNC cells at 1.30 V for thermal cycling tests.

**References**


1. Wu, W. *et al.* 3D Self-Architectured Steam Electrode Enabled Efficient and Durable Hydrogen Production in a Proton-Conducting Solid Oxide Electrolysis Cell at Temperatures Lower Than 600 °C. *Advanced Science* **5**, 1800360 (2018).
2. Wu, W., Zhang, Y., Ding, D. & He, T. A High-Performing Direct Carbon Fuel Cell with a 3D Architectured Anode Operated Below 600 °C. *Advanced Materials* **30**, 1704745 (2018).
3. Bian, W. *et al.* Regulation of Cathode Mass and Charge Transfer by Structural 3D Engineering for Protonic Ceramic Fuel Cell at 400 °C. *Adv Funct Materials* **31**, 2102907 (2021).
4. Tang, W. *et al.* An Unbalanced Battle in Excellence: Revealing Effect of Ni/Co Occupancy on Water Splitting and Oxygen Reduction Reactions in Triple-Conducting Oxides for Protonic Ceramic Electrochemical Cells. *Small* **18**, 2201953 (2022).
5. Duan, C. *et al.* Readily processed protonic ceramic fuel cells with high performance at low temperatures. *Science* **349**, 1321–1326 (2015).
6. Fang, L. *et al.* Boosting the performance of reversible solid oxide electrochemical cells with a novel hybrid oxygen electrode, $Pr_{1.39}Ba_{0.14}Sr_{0.53}Co_{1.48}Fe_{0.76}O_{6-\delta}$-$Ba_{0.66}Sr_{0.34}CoO_{3-\delta}$. *J. Mater. Chem. A* **11**, 21251–21262 (2023).
7. Zheng, S., Bian, W. & Ding, H. A robust protonic ceramic fuel cell with a triple conducting oxygen electrode under accelerated stress tests. *Mater. Adv.* **5**, 2296–2305 (2024).
8. Li, W. *et al.* High performing triple-conductive $Pr_2NiO_{4+\delta}$ anode for proton-conducting steam solid oxide electrolysis cell. *J. Mater. Chem. A* **6**, 18057–18066 (2018).
9. Zhang, X., Zhang, H. & Liu, X. High performance La2NiO4+-infiltrated (La0.6Sr0.4)0.995Co0.2Fe0.8O3− cathode for solid oxide fuel cells. *Journal of Power Sources* **269**, 412–417 (2014).

10. Bi, L. *et al.* Indium as an ideal functional dopant for a proton-conducting solid oxide fuel cell. *International Journal of Hydrogen Energy* **34**, 2421–2425 (2009).
11. Tao, Z., Zhu, Z., Wang, H. & Liu, W. A stable BaCeO3-based proton conductor for intermediate-temperature solid oxide fuel cells. *Journal of Power Sources* **195**, 3481–3484 (2010).
12. Chen, Y. *et al.* Low temperature solid oxide fuel cells with hierarchically porous cathode nano-network. *Nano Energy* **8**, 25–33 (2014).
13. Ishfaq, H. A. *et al.* Boosting performance of the solid oxide fuel cell by facile nano-tailoring of La0.6Sr0.4CoO3-δ cathode. *International Journal of Hydrogen Energy* **47**, 37587–37598 (2022).
14. Namgung, Y., Hong, J., Kumar, A., Lim, D.-K. & Song, S.-J. One step infiltration induced multi-cation oxide nanocatalyst for load proof SOFC application. *Applied Catalysis B: Environmental* **267**, 118374 (2020).
15. Lou, X., Wang, S., Liu, Z., Yang, L. & Liu, M. Improving La0.6Sr0.4Co0.2Fe0.8O3−δ cathode performance by infiltration of a Sm0.5Sr0.5CoO3−δ coating. *Solid State Ionics* **180**, 1285–1289 (2009).
16. Zhao, F., Liu, Q., Wang, S. & Chen, F. Infiltrated multiscale porous cathode for proton-conducting solid oxide fuel cells. *Journal of Power Sources* **196**, 8544–8548 (2011).
17. Lu, C., Sholklapper, T. Z., Jacobson, C. P., Visco, S. J. & De Jonghe, L. C. LSM-YSZ Cathodes with Reaction-Infiltrated Nanoparticles. *J. Electrochem. Soc.* **153**, A1115 (2006).
18. Rehman, S. U. *et al.* Nano-fabrication of a high-performance LaNiO3 cathode for solid oxide fuel cells using an electrochemical route. *Journal of Power Sources* **429**, 97–104 (2019).

19. Tang, W. *et al.* Understanding of A-site deficiency in layered perovskites: promotion of dual reaction kinetics for water oxidation and oxygen reduction in protonic ceramic electrochemical cells. *J. Mater. Chem. A* **8**, 14600–14608 (2020).
20. Kim, D. *et al.* High-Performance Protonic Ceramic Electrochemical Cells. *ACS Energy Lett.* **7**, 2393–2400 (2022).
21. Rajendran, S. *et al.* Tri-Doped $BaCeO_3$ –$BaZrO_3$ as a Chemically Stable Electrolyte with High Proton-Conductivity for Intermediate Temperature Solid Oxide Electrolysis Cells (SOECs). *ACS Appl. Mater. Interfaces* **12**, 38275–38284 (2020).
22. Li, W. *et al.* Layer-structured triple-conducting electrocatalyst for water-splitting in protonic ceramic electrolysis cells: Conductivities vs. activity. *Journal of Power Sources* **495**, 229764 (2021).